Photosystems

DOI: 10.1002/anie.200802590

Photoelectrochemistry with Ordered CdS Nanoparticle/Relay or Photosensitizer/Relay Dyads on DNA Scaffolds**

*Ran Tel-Vered, Omer Yehezkeli, Huseyin Bekir Yildiz, Ofer I. Wilner, and Itamar Willner**

Stepwise vectorial electron transfer from a photoexcited species to an electron acceptor cascade that displays a downhill potential gradient is the fundamental principle in the accomplishment of effective charge separation in natural photosynthesis.[1,2] During the last three decades, extensive research efforts have been directed to adapt the principles of charge separation in the photosynthetic apparatus to artificial systems. Ingenious photosensitizer–electron acceptor chains in covalently linked molecular structures,[3–6] supramolecular structures,[7–9] or organized microenvironments[10–12] have been reported as means to stimulate photoinduced vectorial electron transfer and to accomplish charge separation. The concept of vectorial electron transfer and enhanced charge separation was also adopted in semiconductor nanoparticle systems. Photogeneration of electron–hole pairs in core-shell nanoparticles or hybrid nanoparticles was reported to enhance charge separation by interparticle electron transfer.[13–16] Similarly, the assembly of relay/semiconductor nanoparticle systems on electrodes was reported to provide a means to trap the conduction-band electrons and thus enhance the generation of photocurrents by preventing the electron–hole recombination process at the nanoparticle surface.[17,18]

The sequence of bases in DNA provides instructive functional information that directs, for example, selective hybridization through complementary base pairing, specific cleavage of predesigned duplex domains using endonucleases, sequence-specific recognition and binding of molecular and macromolecular components (e.g. aptamers),[19–21] and the self-organization of sequence-specific catalytic nucleic acids (e.g. DNAzymes).[22,23] Previous studies have demonstrated that duplex DNA structures may act as bridging units that bind semiconductor nanoparticles to electrodes.[24] Similarly, the organization of semiconductor quantum dots/DNA nanostructures was reported.[25] Also, the intercalation of redox-active units into duplex nucleic acids that anchored CdS nanoparticles to electrodes enhanced the generation of photocurrents, and the directions of these photocurrents were reported to be switchable by controlling the redox state of the intercalator.[26] Herein, we report that nucleic acid scaffolds may be used as templates for the structural ordering of relay units and photoactive semiconductor nanoparticles (NPs) or molecular photosensitizers on electrode surfaces. We show that the organization of the components on the DNA templates is essential for the control of charge separation and the resulting photocurrent in the systems, and we demonstrate that the ordering of the components controls the photocurrent direction in the systems. Furthermore, we demonstrate that the association of the nucleic acid tethered photoactive and relay units with the DNA template by hybridization provides a "click-type" method to bind the components in a stepwise manner, exchange the positions of the components on the template, and cleave off predefined components on the DNA by the endonuclease-induced scission of sequence-specific duplex regions.

The two configurations of the relay/CdS NPs nanostructures on the DNA scaffold are shown in Figure 1. The assembly of thiolated nucleic acid **1** on the Au electrode is shown in Figure 1 A. This nucleic acid includes two domains, I and II, which are complementary to the *N*-methyl-*N*′-(2-carboxyethyl)-4,4′-bipyridinium (V^{2+})-functionalized nucleic acid **2**, and to the CdS NP-modified nucleic acid **3**, respectively. The hybridization of **2** and **3** with the template **1**

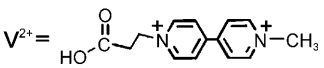

assembles the photoactive NP/relay dyad in the predesigned configuration, where the relay units are positioned between the CdS NPs and the electrode. The second relay/CdS NPs configuration assembled on the DNA template is shown in Figure 1 D. The thiolated DNA template **1** is assembled as a monolayer on the electrode. The domain I is complementary to the CdS NP-functionalized nucleic acid **4**, while domain II is complementary to the V^{2+}-modified nucleic acid **5**. The hybridization of **4** and **5** with the template DNA **1** produces a photoactive NP/relay dyad configuration where the NPs are located close to the electrode and positioned between the relay units and the electrode. These NP/relay configurations include several basic characteristics: 1) the structures are modular and enable the assembly of the CdS NPs without the relay units; thus the effect of the relay units on the photocurrent intensities and directions can be evaluated; and 2) the template **1** and its respective complementary nucleic acids were designed by encoding sequence-specific duplex regions that are cleavable by the endonuclease DdeI. This enables the specific biocatalytic separation of the dyads, as well as the study of the relationship between the NP-dyad structures and the resulting photocurrents.

[*] Dr. R. Tel-Vered, O. Yehezkeli, Dr. H. B. Yildiz, O. I. Wilner, Prof. I. Willner
The Institute of Chemistry, The Hebrew University of Jerusalem
Jerusalem, 91904 (Israel)
Fax: (+972) 2-652-7715
E-mail: willnea@vms.huji.ac.il

[**] This research was supported by the NanoSci-ERA (Nano Licht Project).

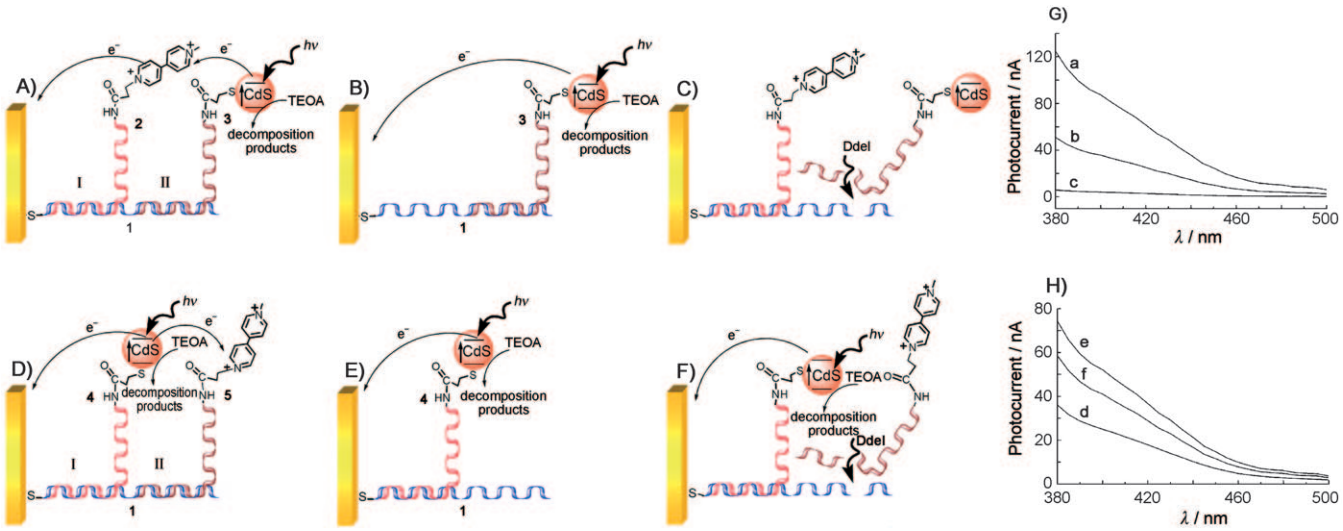

Figure 1. Control of photocurrents in CdS nanoparticle/relay (V^{2+}) dyads assembled on DNA scaffolds linked to electrodes. A) A relay/CdS nanoparticle assembly on a DNA template associated with a Au electrode. B) An assembly containing only CdS-functionalized nucleic acid hybridized to the main scaffold at the remote position with respect to the Au electrode. C) Schematic cleavage of the organized system shown in (A) by DdeI. D) A CdS nanoparticle/relay assembly on a template DNA associated with a Au electrode. E) An assembly containing only the CdS-functionalized nucleic acid hybridized to the main scaffold adjacent to the electrode. F) Schematic cleavage of the organized system shown in (D) by DdeI. G) Photocurrent action spectra generated by: a) The relay/CdS nanoparticle system shown in (A); b) the system assembled in the absence of the V^{2+} relay unit, as shown in (B); c) the system presented in (A), after cleavage with DdeI and the removal of the CdS NP tethered nucleic acid, as is shown in (C). H) Photocurrent action spectra generated by: d) The CdS nanoparticle/relay system shown in (D); e) the system after the exclusion of the remote relay unit, shown in (E); f) the system presented in (D), after treatment with DdeI and the removal of the relay units, as shown in (F). All photocurrents were recorded in phosphate buffer (0.1 M, pH 7.4) that included triethanolamine (20 mM) as a sacrificial electron donor.

The thiolated nucleic acid **1** was immobilized on Au surfaces and its surface coverage was determined to be approximately 3.4×10^{-12} mol cm^{-2} by chronocoulometry[27] using $[Ru(NH_3)_6]^{3+}$ as a label. The bipyridinium-functionalized nucleic acid **2** was hybridized with the DNA template **1**. Coulometric analysis of the redox wave of the V^{2+} units associated with **2** indicated a surface coverage corresponding to 1.1×10^{-12} mol cm^{-2}. The surface coverage of the CdS NPs associated with **3** was characterized by the microgravimetric quartz crystal microbalance (QCM) technique to be 5.4×10^{11} particles cm^{-2}. Figure 1G, curve a, shows the photocurrent action spectrum of the dyad composed of **2** and **3** upon illumination and in the presence of triethanolamine as a sacrificial electron donor. The photocurrent spectrum follows the absorption spectrum of the CdS NPs, which implies that the photocurrent originates from the CdS NPs. Also, no photocurrent was detected in the absence of triethanolamine (TEOA). The direction of the photocurrent was anodic, which indicated that the conduction-band electrons were transported to the DNA-functionalized electrode. Figure 1G, curve b, shows the photocurrent action spectrum of the **1**-functionalized electrode, which included only the hybridized **3**, but without the relay-functionalized nucleic acid **2** (shown in Figure 1B). The resulting photocurrent intensity is approximately 2.5-fold lower than the photocurrent observed in curve a. These results are consistent with the fact that the bipyridinium relay acts as a trap for the conduction-band electrons. This entrapment facilitates the charge separation that is followed by electron transfer, mediated by the bipyridinium relay, to the electrode with the concomitant oxidation of triethanolamine by the valence-band holes. Nevertheless, in the absence of **2**, the direct ejection of the conduction-band electrons into the electrode competes inefficiently with the electron-hole recombination, and yields the low intensity photocurrent, curve b. Figure 1G, curve c, shows the photocurrent that results from the treatment of the duplex structure of **1** with **2** and **3** with DdeI. This confirms the elimination of any photocurrent by cleavage of the photoactive CdS NPs from the scaffold (Figure 1C).

The semiconductor/relay configuration outlined in Figure 1D was characterized in a similar way. The surface coverage of the CdS NPs associated with **4** was found to be approximately 5.1×10^{11} particles cm^{-2} upon hybridization to the scaffold **1**, while the coverage of V^{2+} associated with **5** was approximately 1.0×10^{-12} mole cm^{-2}. Figure 1H, curve e, shows the photocurrent action spectrum observed for the system that includes only **4**, which is hybridized with the DNA template **1** (Figure 1E). The direction of the photocurrent is anodic, which implies that the conduction-band electrons are injected into the electrode. The photocurrent intensity is higher than the value measured upon positioning **3** in the remote site of the scaffold (cf. Figure 1G, curve b), because of the improved charge ejection of the conduction-band electrons to the electrode that arises from the shorter electron-transfer distance. Figure 1H, curve d, shows the photocurrent action spectrum of the composite system consisting of the hybridized assembly between **1**, **4**, and **5** (Figure 1D). In contrast to the previous system, the photocurrent measured in the presence of the bipyridinium-modified nucleic acid relay **5** is substantially lower than the photocurrent measured in the

presence of the CdS NPs alone. Furthermore, the direction of the low-intensity photocurrent is observed to be cathodic. These results are explained by the concomitant operation of different electron-transfer paths of the conduction-band electrons: 1) one path involves the ejection of the photoexcited conduction-band electrons to the bipyridinium relay, which results in a cathodic current, and 2) a competitive path that includes the ejection of the conduction-band electrons to the electrode, with the generation of an anodic photocurrent. The net photocurrent in the system is the result of the oppositely directed photocurrents giving rise to a low-value cathodic current. Treatment of the resulting assembly with the endonuclease DdeI (Figure 1F) results in the scission of the sequence-specific duplex domain of the template and the removal of the nucleic acid tethered bipyridinium relay. The photocurrent spectrum generated by the electrode after treatment with DdeI shows an increase of approximately 60% compared to the photocurrent in the presence of the bipyridinium relay (Figure 1H, curve f). Furthermore, the direction of the photocurrent is found to be anodic. These results are consistent with the cleavage of the bipyridinium relay units, which eliminates the source of the cathodic current. The incomplete recovery of the anodic photocurrent is attributed to incomplete scission of the bipyridinium units from the template.

The generation of photocurrents is not limited to semiconductor nanoparticles; photosensitized electron transfer between photoexcited molecular species and electrodes can be an alternative route for photocurrent generation. Photocurrent enhancements were observed on ITO electrodes modified with porphyrin–fullerene functionalities.[28] Different metal complexes such as metalloporphyrins[29] or Ru^{II} polypyridine complexes[30] have been used as light-harvesting molecules in these systems. The photoinduced electron transfer between photoexcited $[Ru(bpy)_3]^{2+}$ (bpy = 2,2′-bipyridine) and *N*,*N*′-dimethyl-4,4′-bipyridinium (viologen) salts have attracted a great deal of attention in the past three decades.[31] Accordingly, we examined the possibility to construct $[Ru(bpy)_3]^{2+}$–bipyridinium dyads on DNA templates by the nucleic acid hybridization methodology, with the aim to control the photocurrent intensities and their directions by means of the nanoarchitectures associated with the electrodes. The organization of a photosensitizer/relay configuration on the electrode surface is outlined in Figure 2A. The bipyridinium-linked nucleic acid **2** and the $[Ru(bpy)_3]^{2+}$-tethered nucleic acid **6** were hybridized with the DNA template **1**, which was subsequently associated with the electrode. Figure 2G, curve a, shows the photocurrent action spectrum upon illumination of the electrode in the presence of triethanolamine. The photocurrent spectrum follows the UV/Vis spectrum of $[Ru(bpy)_3]^{2+}$, $\lambda_{max} = 455$ nm, and shows an anodic current direction. Control experiments indicated that exclusion of either TEOA or the photosensitizer from the system prohibited the formation of any photocurrent. These results imply that the $[Ru(bpy)_3]^{2+}$ photosensitizer acts as the photoactive component in the system. The oxidative quenching of the excited $[Ru(bpy)_3]^{2+}$ by the bipyridinium electron acceptor results in charge separation and the formation of the bipyridinium radical cation and the oxidized photosensitizer, $[Ru(bpy)_3]^{3+}$. The oxidation of the electron donor TEOA by the oxidized photosensitizer and the concomitant transfer of the electrons from the reduced bipyridinium to the electrode regenerate the dyad configuration, while producing an anodic photocurrent (Figure 2A). Figure 2G, curve b, shows the

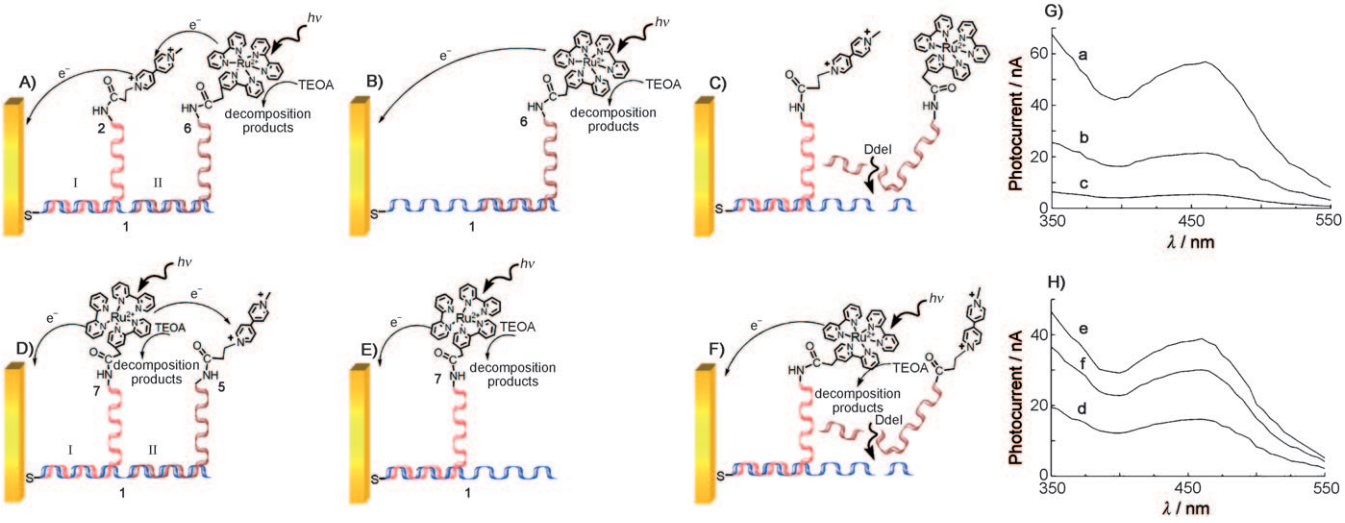

Figure 2. Control of photocurrents by photosensitizer/relay (V^{2+}) dyads assembled on DNA scaffolds linked to electrodes. A) A relay/$[Ru(bpy)_3]^{2+}$ (photosensitizer) assembly on a template DNA associated with a Au electrode. B) An assembly of only a photosensitizer-functionalized nucleic acid hybridized to the scaffold at the remote position with respect to the electrode. C) Schematic cleavage of the organized system shown in (A) by DdeI. D) A photosensitizer/relay assembly on a template DNA associated with a Au electrode. E) An assembly of only the photosensitizer-functionalized nucleic acid adjacent to the electrode. F) Cleavage of the system shown in (D) by DdeI. G) Photocurrent action spectra generated by: a) The relay/photosensitizer system shown in (A); b) the system presented in (B); c) the system presented in (A), after cleavage with DdeI and the removal of the photosensitizer, as shown in (C). H) Photocurrent action spectra generated by: d) The photosensitizer/relay system shown in (D); e) the system presented in (E); f) the system presented in (D), after treatment with DdeI and the removal of the relay units, as shown in (F). Photocurrents were recorded in phosphate buffer (pH 7.4, 0.1 M) that included triethanolamine (20 mM) as a sacrificial electron donor.

photocurrent spectrum observed upon the exclusion of the bipyridinium electron acceptor unit from the DNA template (Figure 2B). The intensity of the photocurrent decreases, which is consistent with the fact that the stepwise electron transfer from the excited $[Ru(bpy)_3]^{2+}$ to the bipyridinium relay unit is eliminated, and thus charge separation does not proceed. The duplex region that links the $[Ru(bpy)_3]^{2+}$ photosensitizer to the DNA template includes the cleavable sequence by DdeI. Upon treatment of the supramolecular photosensitizer–bipyridinium assembly with DdeI (Figure 2C), the resulting photocurrent (Figure 2G, curve c) is almost depleted, which is consistent with the removal of the photoactive units. The residual photocurrent is attributed to the incomplete cleavage of the photosensitizer from the template structure.

The second configuration of the $[Ru(bpy)_3]^{2+}$–bipyridinium assembly involved the positioning of the photosensitizer units close to the electrode by the hybridization of the $[Ru(bpy)_3]^{2+}$-tethered nucleic acid **7** to the electrode, as well as positioning the bipyridinium-tethered nucleic acid **5** at the remote site on the DNA template (Figure 2D). Figure 2H, curve d, shows the photocurrent that occurs upon illumination of the assembly in the presence of TEOA. In contrast to the previous configurations, where an anodic photocurrent was observed, the net photocurrent occurred in the cathodic direction in this case. Figure 2H, curve e, shows that an enhanced anodic photocurrent is obtained in the absence of the bipyridinium electron relay. Also, treatment of the assembly with DdeI facilitated a partial removal of the bipyridinium relay from the structure by scission of the sequence-specific region, which resulted in the increase of the photocurrent (Figure 2H, curve f). These results imply that the photosensitizer units transfer electrons to the bipyridinium sites, and the oxidized photosensitizer is subsequently reduced by TEOA to regenerate the photoactive component. It should be emphasized that the photocurrent generated in the assembly described in Figure 2B is lower than the photocurrent generated by the system where the photosensitizer was positioned on the DNA template near the electrode (Figure 2E), which confirms the smaller distance between the photosensitizer and the electrode in this configuration.

In conclusion, the present study has demonstrated the organization of semiconductor NP/relay or photosensitizer/electron-acceptor structures on electrodes by their programmed assembly on DNA templates linked to electrode surfaces. The exact composition and orientation of the nanostructures controlled the intensities and directions of the resulting photocurrents. From the number of bases in the DNA sequences, we estimate the length of the template **1** to be approximately 11 nm. It should be noted that the flexibility of the single-stranded nucleic acid tethers carrying the bipyridinium electron relay, the CdS NPs, or the photosensitizer prevents us from any detailed considerations of distance effects on the photocurrent efficiencies, and only the relative positions of the components control the resulting intensities of the photocurrents and their directions. The concept that we introduce may be extended beyond photoelectrochemistry, and the assembly of enzyme cascades or sequential electron transfer along (bio)molecular arrays on the DNA scaffold may be envisaged.

Experimental Section

CdS nanoparticles: The CdS NPs were prepared by the reverse micellar method as described before.[32] Thiol-capped CdS NPs were prepared by the addition of aqueous solutions of 3-mercaptopropane sulfonic acid sodium salt (396 μL, 0.32 M) and mercaptopropionic acid (66 μL, 0.32 M) into the micellar nanoparticle solution, and the resulting mixture was stirred for 14 h under argon. Pyridine (20 mL) was then added, and the resulting precipitate was washed with *n*-heptane, petroleum ether, butanol, and methanol. An average particle size of 8.5 nm was estimated by transmission electron microscopy (TEM). Photoelectrochemical experiments were performed on a home-built instrument described previously.[18]

Dyad assembly: The following nucleic acid sequences, containing amine terminals at the 5′-position, were purchased from Sigma:
Sequence 1: HS-AAAAAGTGAGTGAGTGAACCTCAGCAATA
Sequence 2: NH_2-AAAAAAAAAAAAAAATCACTCACTCAC
Sequence 3: NH_2-AAAAAAAAAATATTGCTGAGGT

The nucleic acid sequences 2 and 3 (5 μM) were modified with an excess of either: mercaptopropionic acid functionalized CdS nanoparticles, $[Ru(bpy)_2$(4-(2,2′-bipy acetic acid *N*-succinimidyl ester)$]PF_6$, or *N*-methyl-*N*′-(2-carboxyethyl)-4,4′-bipyridinium, according to the desired configuration. The different functionalities were bound to the amine terminals of the DNA sequences by immersion in a 4-(2-hydroxyethyl)-1-piperazinyl ethanesulfonic acid (HEPES) buffer solution (10 mM, pH 7.2) containing 1-ethyl-3-(3-dimethylaminopropyl)carbodiimide (EDC, 10 mM) and *N*-hydroxysuccinimide (NHS, 10 mM) for 2 h, followed by separation of the product in a microspin (G-25) column. The modified DNA sequences were hybridized for 20 min in a HEPES buffer solution (10 mM) containing NaCl (0.3 M), with the main scaffold (DNA sequence 1), followed by treatment with 1,4-dithio-threitol (DTT) for 2 h and separation by a microspin column. The resulting hybridized DNA structure was adsorbed onto a clean Au wire electrode ($d = 0.5$ mm) for 1.5 h through the thiol terminal associated with the main scaffold (sequence 1). The electrodes were carefully washed with HEPES buffer to ensure the removal of any nonspecifically adsorbed DNA molecules. Cleavage experiments employed a DdeI enzyme (BioLabs Inc., 1×10^4 units mL^{-1}) in a tris(hydroxymethyl)aminomethane (TRIS) buffer (50 mM at pH 7.9) containing $MgCl_2$ (10 mM) and NaCl (100 mM).

Received: June 3, 2008
Revised: July 27, 2008
Published online: September 22, 2008

Keywords: DNA · nanoparticles · photocurrent · photoelectrochemistry · photosensitizer · semiconductors

[1] I. Willner, B. Willner, *Coord. Chem. Rev.* **2003**, *245*, 139–151.
[2] M. R. Wasielewski, *Chem. Rev.* **1992**, *92*, 435–461.
[3] T. A. Moore, D. Gust, P. Mathis, J. C. Mialocq, C. Chachaty, R. V. Bensasson, E. J. Land, D. Doizi, P. A. Liddell, W. R. Lehman, G. A. Nemeth, A. L. Moore, *Nature* **1984**, *307*, 630–632.
[4] S. L. Mecklenburg, B. M. Peek, B. W. Erickson, T. J. Meyer, *J. Am. Chem. Soc.* **1991**, *113*, 8540–8542.
[5] D. Gust, T. A. Moore, A. L. Moore, D. Barrett, L. O. Harding, L. R. Makings, P. A. Liddell, F. C. De Schryver, M. Van der Auweraer, R. V. Bensasson, M. Rougee, *J. Am. Chem. Soc.* **1988**, *110*, 321–323.
[6] M. R. Wasielewski, M. P. Niemczyk, W. A. Svec, E. B. Pewitt, *J. Am. Chem. Soc.* **1985**, *107*, 5562–5563.

[7] M. Seiler, H. Dürr, I. Willner, E. Joselevich, A. Doron, J. F. Stoddart, *J. Am. Chem. Soc.* **1994**, *116*, 3399 – 3904.
[8] M. Kropf, E. Joselevich, H. Dürr, I. Willner, *J. Am. Chem. Soc.* **1996**, *118*, 655 – 665.
[9] E. Zahavy, M. Seiler, S. Marx-Tibbon, E. Joselevich, I. Willner, H. Dürr, D. O'Connor, A. Harriman, *Angew. Chem.* **1995**, *107*, 1112 – 1115; *Angew. Chem. Int. Ed. Engl.* **1995**, *34*, 1005 – 1008.
[10] J. S. Krueger, J. E. Mayer, T. E. Mallouk, *J. Am. Chem. Soc.* **1988**, *110*, 8232 – 8234.
[11] I. Willner, J. M. Yang, J. W. Otvos, M. J. Calvin, *J. Phys. Chem.* **1981**, *85*, 3277 – 3283.
[12] P.-A. Brugger, P. P. Infelta, A. M. Braun, M. Grätzel, *J. Am. Chem. Soc.* **1981**, *103*, 320 – 326.
[13] P. Yu, K. Zhu, A. G. Norman, S. Ferrere, A. J. Frank, A. J. Nozik, *J. Phys. Chem. B* **2006**, *110*, 25451 – 25454.
[14] I. Robel, V. Subramanian, M. Kuno, P. V. Kamat, *J. Am. Chem. Soc.* **2006**, *128*, 2385 – 2393.
[15] C. Nasr, S. Hotchandani, W. Y. Kim, R. H. Schmehl, P. V. Kamat, *J. Phys. Chem. B* **1997**, *101*, 7480 – 7487.
[16] A. Zaban, S. G. Chen, S. Chappel, B. A. Gregg, *Chem. Commun.* **2000**, 2231 – 2232.
[17] L. Sheeney-Haj-Ichia, J. Wassermann, I. Willner, *Adv. Mater.* **2002**, *14*, 1323 – 1326.
[18] L. Sheeney-Haj-Ichia, I. Willner, *J. Phys. Chem. B* **2002**, *106*, 13094 – 13097.
[19] A. D. Ellington, J. W. Szostak, *Nature* **1990**, *346*, 818 – 822.
[20] E. N. Brody, L. Gold, *Rev. Mol. Biotechnol.* **2000**, *74*, 5 – 13.
[21] C. Tuerk, L. Gold, *Science* **1990**, *249*, 505 – 510.
[22] R. R. Breaker, *Nat. Biotechnol.* **1997**, *15*, 427 – 431.
[23] R. R. Breaker, *Curr. Opin. Chem. Biol.* **1997**, *1*, 26 – 31.
[24] I. Willner, F. Patolsky, J. Wasserman, *Angew. Chem.* **2001**, *113*, 1913 – 1916; *Angew. Chem. Int. Ed.* **2001**, *40*, 1861 – 1864.
[25] a) J. Sharma, Y. Ke, C. Lin, R. Chhabra, Q. Wang, J. Nangreave, Y. Liu, H. Yan, *Angew. Chem.* **2008**, *120*, 5235 – 5237; *Angew. Chem. Int. Ed.* **2008**, *47*, 5157 – 5159; b) A. Fu, C. M. Micheel, J. Cha, H. Chang, H. Yang, A. P. Alivisatos, *J. Am. Chem. Soc.* **2004**, *126*, 10832 – 10833.
[26] R. Gill, F. Patolsky, E. Katz, I. Willner, *Angew. Chem.* **2005**, *117*, 4630 – 4633; *Angew. Chem. Int. Ed.* **2005**, *44*, 4554 – 4557.
[27] A. B. Steel, T. M. Herne, M. Tarlov, *J. Anal. Chem.* **1998**, *70*, 4670 – 4677.
[28] H. Yamada, H. Imahori, Y. Nishimura, I. Yamazaki, S. Fukuzumi, *Adv. Mater.* **2002**, *14*, 892 – 895.
[29] M. Lahav, T. Gabriel, A. N. Shipway, I. Willner, *J. Am. Chem. Soc.* **1999**, *121*, 258 – 259.
[30] M. Lahav, V. Heleg-Shabtai, J. Wasserman, E. Katz, I. Willner, H. Dürr, Y. Hu, S. H. Bossmann, *J. Am. Chem. Soc.* **2000**, *122*, 11480 – 11487.
[31] S. Campagna, F. Puntotiero, F. Nastasi, G. Bergamini, V. Balzani, *Top. Curr. Chem.* **2007**, *280*, 117 – 214.
[32] E. Granot, F. Patolsky, I. Willner, *J. Phys. Chem. B* **2004**, *108*, 5875 – 5881.

